Atomic and Molecular Photoabsorption

ABSOLUTE TOTAL CROSS SECTIONS

Joseph Berkowitz

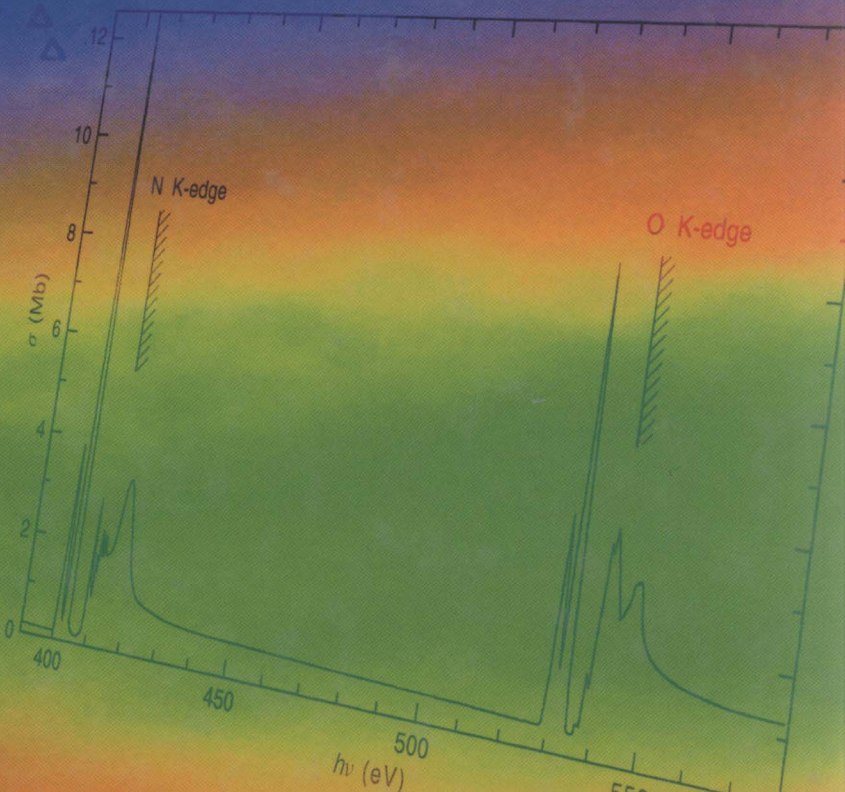

Atomic and Molecular Photoabsorption

Absolute Total Cross Sections

Joseph Berkowitz
Argonne National Laboratory,
Argonne, IL 60439, USA

ACADEMIC PRESS
A Division of Harcourt, Inc.
San Diego San Francisco New York Boston
London Sydney Tokyo

This book is printed on acid-free paper.

Academic Press
A Division of Harcourt, Inc.
Harcourt Place, 32 Jamestown Road, London NW1 7BY, UK
http://www.academicpress.com

Academic Press
A Division of Harcourt, Inc.
525 B Street, Suite 1900, San Diego, California 92101-4495, USA
http://www.academicpress.com

ISBN 0-12-091841-2

Library of Congress Catalog Number: 2001088743

A catalogue record for this book is available from the British Library

Typeset by Laser Words Pvt. Ltd., Chennai, India
Printed and bound in Great Britain by MPG Books, Bodmin, Cornwall

01 02 03 04 05 06 07 MP 9 8 7 6 5 4 3 2 1

Atomic and Molecular Photoabsorption

Absolute Total Cross Sections

Acknowledgment

The author wishes to express his gratitude to Dr. Mitio Inokuti of Argonne National Laboratory, who has been unstinting of his time while sharing his extensive knowledge of several topics in this monograph. He is also thankful to Dr. Inokuti for accepting the onerous task of reading and commenting on the manuscript.

Contents

1
Introduction

1.1 Introduction

Is there ever an optimum time to review an active field of research? For the present topic, a critical evaluation requires a significant investment of time. During this interval, additional information becomes available. One tries to compensate, but it is a series without a convergence limit.

Two decades ago, this author made such an effort (Berkowitz, 1979) at a time when electron synchrotrons were mostly first generation. Even though the field was developing rapidly, general principles could be presented, and one could broadly map the landscape. In the intervening time, new technology and improved calculational capability (and also more experimental sites, more researchers) have vastly increased the available information. It was predictable that increased light intensity from second- and third-generation synchrotrons would enable more difficult, differential cross sections to be measured. But improvements have also been realized in the determination of absolute total cross sections. In the high-energy region, prior data were largely confined to x-ray lines, but currently the smooth continuum emanating from synchrotrons can map out the structure in the vicinity of K- and L-edges of atoms and molecules. In the vacuum ultraviolet, early synchrotron data were encumbered by scattered light and second-order radiation, but more recent experiments, particularly by Holland and collaborators, appear to have overcome these problems. Samson and collaborators have largely avoided such potential uncertainties by using a many-line spark source, and with improved measurement techniques have reduced their combined statistical and systematic error to 1–3%.

Very sharp structure occurs in the photoabsorption spectra of small (usually di- and tri-atomic) molecules in the sub-ionization region. This can lead to saturation at peaks in photoabsorption measurements, if the instrumental resolution is broader than the inherent line width, in experiments based on the Beer–Lambert law. Inelastic energy loss experiments, employing a thin target, effectively avoid saturation, although their resolution is typically poorer than optical studies. Hence, they can provide a check on optical measurements where saturation is possible. Brion and collaborators have recently published a summary of their (e,e) data. Our practice is to utilize photoabsorption measurements when problems such as saturation can be avoided, since the electron energy loss data

require an auxiliary normalization (such as the Thomas–Reiche–Kuhn sum rule (TRK) for $S(0)$), which implies a redundancy, since we are utilizing the sum rules to make selections from available data. In some instances (He, H_2), accurate calculations of sub-ionization oscillator strengths are available.

In the earlier volume (Berkowitz, 1979), attention was focused on three sum rules, $S(-2)$, $S(-1)$ and $S(0)$. See 1.2 Reference Table for definitions of $S(p)$. Here, we have extended the study to include $S(+1)$ and $S(+2)$, which emphasize energies typically beyond K-edges. At these high energies, the electric dipole photoabsorption cross section continues to decline precipitously (as $\sim E^{-3.5}$) and higher-order processes (particularly Rayleigh and Compton scattering) begin to dominate. The very low cross sections make measurements difficult. The conventional experiment in the past has measured attenuation, which is the sum of photoabsorption and scattering processes. The photoabsorption component has been inferred by subtracting calculated scattering cross sections from the photoattenuation cross section. The uncertainty can be large, when the subtracted component is >90% of photoattenuation (see, e.g., the helium section). Experiments with third-generation synchrotrons are currently being undertaken to directly determine the individual contributions. The expectation value of $S(+2)$ can play an important role, since it is related to the photoabsorption component alone.

The expectation value for $S(+2)$ is proportional to the electron density at the nucleus. Atomic Hartree–Fock calculations provide this quantity rather accurately. Equivalent calculations for N_2 and O_2 demonstrate that atomic additivity works quite well. We shall find empirically that it is generally a good approximation for molecules. It is not as good for $S(+1)$, where a term dependent upon correlation enters into the expectation value equation (see Reference Table for sum rules).

As implied above, direct measurements of photoabsorption cross sections above ~30 keV are scarce and uncertain. Of necessity, we invoke calculated values. Between 10^4–10^5 eV, we avail ourselves of the recently tabulated, calculated atomic photoabsorption cross sections of Chantler (1995). At these high energies, molecular cross sections can be accurately approximated as atomic sums for the relatively low Z atoms considered. For $h\nu > 10^5$ eV, we have calculated atomic cross sections using a hydrogenic equation with screening given by Bethe and Salpeter (1977). It is non-relativistic, assumes only electric dipole processes, and applies only to K shells. At 10^5 eV, we have compared the atomic cross sections provided by this equation with the calculated values of Chantler and the 'photoelectric' cross sections given by Hubbell (1969) for selected atoms, and find very good agreement. However, at higher energies Hubbell's cross sections rapidly exceed the hydrogenic formula, presumably because they contain relativistic and non-dipole effects. They may be more physically realistic, but their spectral sum would be inconsistent with the expectation values (especially for $S(+2)$), since the derivation of these sum rules implies non-relativistic, electric dipole photoabsorption. Specifically, the equation we use for all cases except He

and H_2 (which require special consideration) is

$$\sigma = 6.8 \times 10^{-16}(Z - 0.3)^6(Ry/\nu)^4 f(\chi),$$

where σ is in cm^2, Z the atomic number, Ry = Rydberg, $\chi = \sqrt{\nu_1/(\nu - \nu_1)}$ and $f(\chi) = \exp(-4\chi)\arctan(1/\chi)/1 - \exp(-2\pi\chi)$. Here, ν is the running photon frequency, and ν_1 corresponds to the K-edge. At energies well above the K-edge, the experimental value of ν_1 can be used.

After evaluating these cross sections, we compute $S(p)$, $0 \leq p \leq 2$, for successive decades of energy between 10^5–10^9 eV, and record these values for each system. Only at $h\nu \sim 10^9$ eV does asymptotic behavior $\sigma \propto E^{-3.5}$ manifest itself. We demonstrate this by fitting these very high-energy cross sections to an appropriate expansion, $\sigma \propto AE^{-3.5} + BE^{-4.0} + CE^{-4.5}$, and find that the first term dominates. This expansion permits analytical integration from $10^9 < h\nu <$ infinity. The resulting values of $S(+2)$ are usually within 2% of the 'expectation' values.

Some may object to using the term 'expectation value' in this context, since it is usually reserved for describing the eigenvalue of an operator, or equivalently, a matrix element. We justify its use here because (apart from $S(-2)$) the $S(p)$ are matrix elements, multiplied by constants. Other terms, such as 'expected value' or 'anticipated value' fall short of conveying the intended meaning.

The expectation value for $S(-2)$ is proportional to the electric dipole polarizability, more specifically the static polarizability. Compared to Berkowitz (1979), more careful attention has been given to data sources, and to the occasionally important infrared contribution, which should not be included in the current comparisons. Bishop and Cheung (1982) summarized available information on this topic for a number of molecules considered in this monograph. Among the alkali atoms, the resonance transition typically accounts for approximately 99% of the polarizability. Recently, some impressive experiments have provided accurate oscillator strengths for these transitions. At least as noteworthy is a measurement of the electric dipole polarizability of sodium by Pritchard and collaborators (Ekstrom *et al.*, 1995), in which two interfering atomic beams are used as an interferometer.

In addition to lithium and sodium, we include atomic nitrogen, oxygen, chlorine, ozone and C_{60} in this monograph. Berkowitz (1979) was largely confined to permanent gases and vapors with sufficient vapor pressure at room temperature to enable Beer's law measurements. This excluded most atoms, and the large class of transient molecular species. New techniques of calibration have been reported recently for calibrating the absolute cross sections of high-temperature vapors. For others, typified by N, O and Cl, experimentalists have tried to exploit specific techniques related to the method of generation. Needless to say, the uncertainties here are much larger than with permanent gases. For even the simplest, relatively stable transient molecular species, the available data were judged too fragmentary for inclusion.

Modern ab initio calculations (many-body perturbation theory, random phase approximation with exchange, R-matrix) have become increasingly useful for atoms, supplementing and in some cases correcting experimental cross sections. Recent applications to open-shell atoms are particularly welcome, because of the aforementioned calibration problems. Thus far, calculations for molecules other than H_2 have been less successful. Special mention should be made of the highly correlated wave functions which have been used to calculate $S(p)$ for He, Li and H_2.

In the past 10–15 years, W. J. Meath and collaborators have presented their distribution of oscillator strengths for many of the atoms and molecules presented here. Their approach is a constrained optimization procedure based on Lagrange multiplier techniques. Various sources of input data are used, subject to satisfying experimental molar refractivities (related to $S(-2)$) and the TRK sum rule. The results are presented as integrated oscillator strengths encompassing various energy intervals. The procedure will generally alter the input data, sometimes beyond the stated experimental uncertainty. It is not unique, since it depends upon the input data available. They stress that their dipole oscillator strength distributions (DOSDs) are not totally reliable in local detail, since the constraint procedures 'cannot completely offset the errors that are inherent in the input information'.

Our goal is somewhat different. We wish to find the best local cross sections, using the sum rules as a guide. This can be very important in regions of sharp structure, where the experimental resolution can influence the maximum and minimum cross section. Some initial filtering of older and/or less precise data is performed, and where necessary, subjective judgments are made, based on the track record of the experimental group. Numerous graphical comparisons are presented. Atomic additivity is employed where related experiments have established its validity, typically in regions devoid of structure. Where possible, direct measurements rather than mixture rules are used in regions displaying structure near K- or L-edges. In many instances newer, and usually more precise data have become available and are incorporated. The presentation is intended to enable the reader to find the best choice of photoabsorption cross sections for the specified system at any given energy.

This information can be utilized to evaluate properties other than the moments of the oscillator strength distribution $S(p)$. These include four differently weighted averages of $\ln E_n$, which we represent compactly (Fano and Cooper, 1968)

$$\ln I(p) = \sum_n E_n^p (\ln E_n) f_n / S(p)$$

They concern the total inelastic scattering cross section for grazing collisions of fast-charged particles with the target species ($p = -1$), the average energy loss, or stopping power in these collisions ($p = 0$), its mean fluctuation ($p = 1$) and the Lamb shift ($p = 2$). The lower energy range of the oscillator strength distribution may be used to estimate the C_6 constant for intermolecular van der Waals interactions.

A related goal is to determine absolute partial cross sections, which can involve states of the ion, stages of ionization, or (with molecules) the abundance of different fragments. The latter measurements are usually presented as branching ratios, e.g., in photoelectron spectroscopy or photoionization mass spectrometry, but can be placed on an absolute scale using absolute photoionization cross sections. For atoms, there is practically little distinction between photoabsorption and photoionization cross sections, except in isolated cases where autoionization may be restricted by selection rules. With molecules, there is usually a region between the ionization potential and roughly 20 eV where other mechanisms, typically direct dissociation and predissociation, compete with direct ionization and autoionization. Hence, auxiliary measurements are required to determine the fractional ionization, referred to as the quantum yield of ionization η_i. In this monograph, we devote an entire chapter to a survey of the mechanisms underlying η_i for various molecules, and we attempt to rationalize why η_i approaches unity at $\sim$20 eV for all molecules studied, regardless of size. The totality of ionizations at all energies is related to the absolute ionization cross section for electron impact at very high energies (see Berkowitz (1979)), and comparisons between those two different experiments are made here.

In recent years, a technique called ZEKE (zero electron kinetic energy) has been introduced in photoionization studies. Pulsed laser radiation, involving one or more photons, excites atoms or molecules to within $<10^{-3}$ eV of the first (or higher) ionization potential. After a short delay, a weak electric field induces ionization by the Stark effect. In the present study, our primary interest in ZEKE is that it can provide precise ionization potentials, which mark a convenient separation of photoabsorption/photoionization processes. It has been found that the states probed by ZEKE are longer-lived than expected for high n, low ℓ excited states. Two conflicting views of this long lifetime were presented, one involving dispersion of initially low ℓ states to the entire ℓ (and m_ℓ) manifold by the presence of weak external fields and ions, the other invoking an interaction between the high Rydberg electron and the core. Currently, experiments favor the former as an explanation for the long ZEKE lifetimes, but the latter is almost certainly involved in determining the quantum yield of ionization. It is an intrinsic property of the molecule, and potentially holds greater interest than environmental (electric field, point charge) effects.

This monograph terminates at $Z = 18$, both because detailed absolute photoabsorption cross sections are less complete for atoms and molecules of heavier atoms, and because the sum rules may begin to depart from the formulas given in the Reference Table, due to relativistic effects and higher multipole effects. These sum rules are based on electric-dipole-allowed transitions. Recently, considerable attention has been directed at non-dipolar effects, at photon energies as low as several hundred eV. They are observed as backward-forward asymmetries in photoelectron angular distributions, and arise from cross terms (electric dipole-electric quadrupole, E1-E2, and electric dipole-magnetic dipole, E1-M1) in the multipole expansion of the incident electromagnetic wave. In photoabsorption,

only even multiples occur in the expansion; the influence on the sum rules is negligible for low Z, and for incident wavelengths much longer than orbital dimensions.

1.2 Reference Table: Sum Rules (Rydberg Units)†

	Spectral sum	Expectation value
$S(-2)$	$\sum_n f_n/E_n^2 + \int_{\text{IP}}^{\infty} (1/E^2)(\mathrm{d}f/\mathrm{d}E)\,\mathrm{d}E$	$\alpha/4a_0^3$
$S(-1)$	$\sum_n f_n/E_n + \int_{\text{IP}}^{\infty} (1/E)(\mathrm{d}f/\mathrm{d}E)\,\mathrm{d}E$	$\left\langle 0 \left\vert \left(\sum_i^N r_i\right)^2 \right\vert 0 \right\rangle \Big/ 3$
$S(0)$	$\sum_n f_n + \int_{\text{IP}}^{\infty} (\mathrm{d}f/\mathrm{d}E)\,\mathrm{d}E$	N
$S(+1)$	$\sum_n f_n \cdot E_n + \int_{\text{IP}}^{\infty} E(\mathrm{d}f/\mathrm{d}E)\,\mathrm{d}E$	$(4/3)\left\{ E_0 + 1/2 \sum_{i\neq j} (0\vert p_i \cdot p_j \vert 0) \right\}$
		$= 4/3 \left\langle 0 \left\vert \left(\sum_{i=l}^N p_i\right)^2 \right\vert 0 \right\rangle$
$S(+2)$	$\sum_n f_n \cdot E_n^2 + \int_{\text{IP}}^{\infty} E^2(\mathrm{d}f/\mathrm{d}E)\,\mathrm{d}E$	$(16\pi/3) \sum_a Z_a \left\langle 0 \left\vert \sum_{i=l}^N \delta(r_{ia}) \right\vert 0 \right\rangle$

In most molecules and some atoms, individual transitions below the IP may not be resolved. The summation must then be replaced by an integral.

The expectation values are for neutral atoms and molecules. They are derived with a non-relativistic Hamiltonian, with transitions confined to the dipole approximation. The nuclei are considered point charges at fixed positions. For non-spherical species, the expectation value is an average over orientations. The polarizability α related to $S(-2)$ is the static electric dipole polarizability, determined from electronic transitions, and sometimes referred to as α^{uv}. Some experiments yield $\alpha^{\text{tot}} = \alpha^{\text{ir}} + \alpha^{\text{uv}}$, where α^{ir} is the contribution of vibrational excitations in the infrared.

Hirschfelder *et al.* (1964) provide a more detailed description of these sum rules, applicable to molecules as well as atoms, and incorporating the finite mass of the nuclei. For $S(0)$, the correction is of order m/m_α, and for $S(+2)$, of order $(m/m_\alpha)^2$, where m = electron mass, m_α = nuclear mass. When applied to H_2, $S(0)$ becomes 2.001 (0.05% correction), and proportionately much less for $S(+2)$. For $S(-1)$ and $S(+1)$ the corrections are less transparent, but we shall rarely encounter sufficiently accurate ab initio calculations of these expectation values to warrant concern. On the other hand, we use $S(0) = N$, the Thomas–Reiche–Kuhn sum rule, which should be accurate to ~0.1%.

Definitions

f = oscillator strength (dimensionless)
E = energy (Rydbergs)
α = polarizability (cm^3)
a_0 = Bohr radius (cm^3)
r_i = vector position of i^{th} electron
N = total no. of electrons
E_0 = total electron kinetic energy
p_i, p_j = momentum vector of i^{th}, j^{th} electron
Z_a = nuclear charge of a^{th} nucleus
$\delta(r_{ia})$ = charge density of i^{th} electron at nucleus a

†See, e.g. Dalgarno and Lynn (1957); Bethe and Salpeter (1977) p. 358

Conversion Factors

σ(Mb) = 109.760 97 (41) Mb eV (df/dE)
σ(Mb) = 8.067 283 (64) Mb Ryd ($df/d(E/R)$)
eV · Å = 12 398.418 57 (49)

2
Atoms

2.1 Atomic Hydrogen

These absolute cross sections are known more accurately from theory than experiment, and are included here for completeness. The values of $S(+2)$ and $S(+1)$ are utilized in the estimation of hydrogen-containing molecules (except H_2) by summing atomic quantities.

The oscillator strengths for the Lyman series ($1s \rightarrow np$) are given by Bethe and Salpeter (1971, p. 263).

$$f_n = \frac{2^8 n^5 (n-1)^{2n-4}}{3(n+1)^{2n+4}}$$

These oscillator strengths, and the corresponding transition energies, are given explicitly by Morton (1991) and also Verner *et al.* (1994) to $n = 30$.

The ionization potential of atomic hydrogen is 13.598 44 eV. The oscillator strength distribution in the continuum is given by

$$df/d\varepsilon = (2^7/3)(1+k^2)^{-4} \exp\left(\frac{4}{k}\arctan k\right)[1-\exp(-2\pi/k)]^{-1},$$

where $\varepsilon = k^2$ is the electron kinetic energy, and the incident photon energy $E = 1 + \varepsilon$. Dillon and Inokuti (1981) have derived a 5-term series expansion for the above expression, accurate to 1% for $0 < \varepsilon < 5$, or $h\nu$ up to 81.63 eV. Figure 2.1 is a histogram showing how $\Delta f/\Delta E$ smoothly merges with df/dE at the onset of the continuum.

The values of $S(p)$, in Rydberg units, are: $S(-2) = 9/8$, $S(-1) = 1.0$, $S(0) = 1.0$, $S(+1) = 4/3$ and $S(+2) = 16/3$.

2.2 Helium

Helium warrants special consideration, because one anticipates a closer concordance between the spectral distribution of oscillator strengths with sum rules than with all other systems except atomic hydrogen. Here, calculated values surpass experimental results in accuracy in almost all spectral regions. Indeed, helium has been a veritable proving ground for various theories incorporating correlation. At

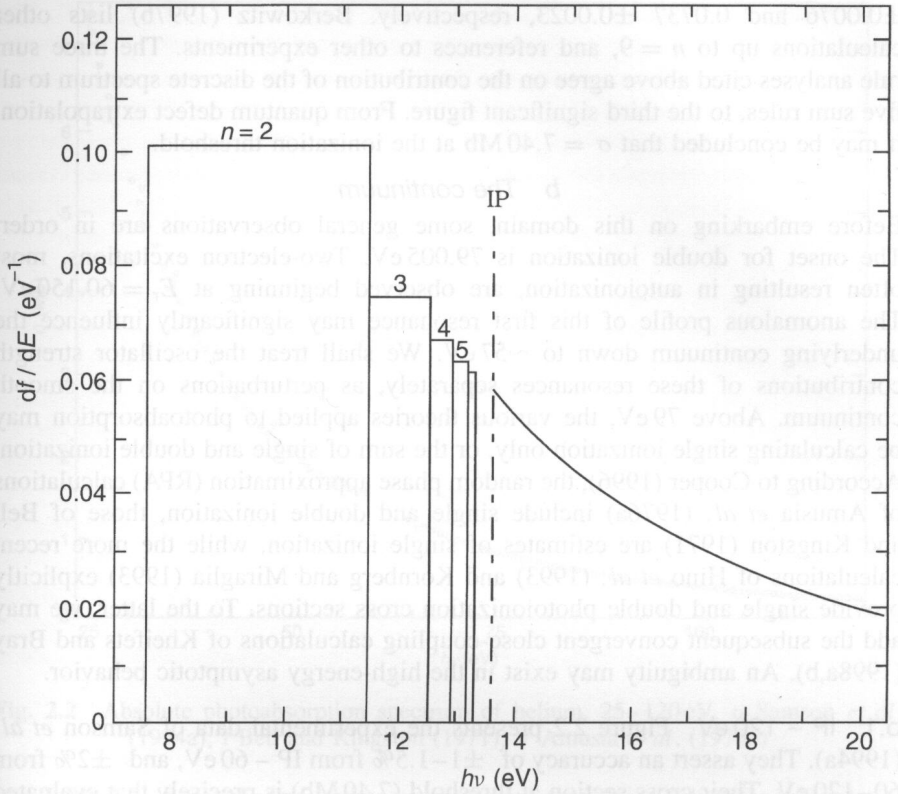

Fig. 2.1 A histogram displaying the convergence of the average oscillator strength in the discrete spectrum to the continuum cross section at the IP, for atomic hydrogen

least three sum rule analyses (Cooper, 1996; Berkowitz, 1997b; Yan *et al*., 1998) have been reported in recent years. We shall focus on the areas of agreement and disagreement, and try to elicit the best current values.

2.2.1 The data

The ionization potential of helium, based on spectral analysis, is 198 310.7745(40) cm^{-1}, or 24.587 399 89(50) eV (Martin, 1984). Recent Lamb shift experiments obtained 198 310.6672(15) cm^{-1} (Eikema *et al*., 1997) and 198 310.6711(16) cm^{-1} (Bergeson *et al*., 1998).

a The discrete spectrum

Already in 1971, Schiff *et al*. (1971) calculated the oscillator strengths of the lowest four transitions ($1s^2 \rightarrow 1snp$, $n = 2$–5) to high precision. For the first two, they obtained 0.2762 and 0.0734. Recently, Drake (1996) calculated 0.276 164 7 and 0.073 434 9. Experimentally, Gibson and Risley (1995) determined 0.2700

±0.0076 and 0.0737 ±0.0023, respectively. Berkowitz (1997b) lists other calculations up to $n = 9$, and references to other experiments. The three sum rule analyses cited above agree on the contribution of the discrete spectrum to all five sum rules, to the third significant figure. From quantum defect extrapolation, it may be concluded that $\sigma = 7.40$ Mb at the ionization threshold.

b The continuum

Before embarking on this domain, some general observations are in order. The onset for double ionization is 79.005 eV. Two-electron excitations, most often resulting in autoionization, are observed beginning at $E_r = 60.150$ eV. The anomalous profile of this first resonance may significantly influence the underlying continuum down to ~57 eV. We shall treat the oscillator strength contributions of these resonances separately, as perturbations on the smooth continuum. Above 79 eV, the various theories applied to photoabsorption may be calculating single ionization only, or the sum of single and double ionization. According to Cooper (1996), the random phase approximation (RPA) calculations of Amusia *et al*. (1976a) include single and double ionization, those of Bell and Kingston (1971) are estimates of single ionization, while the more recent calculations of Hino *et al*. (1993) and Kornberg and Miraglia (1993) explicitly provide single and double photoionization cross sections. To the latter, we may add the subsequent convergent close-coupling calculations of Kheifets and Bray (1998a,b). An ambiguity may exist in the high-energy asymptotic behavior.

b.1 IP – 120 eV Figure 2.2 presents the experimental data of Samson *et al*. (1994a). They assert an accuracy of ±1–1.5% from IP – 60 eV, and ±2% from 60–120 eV. Their cross section at threshold (7.40 Mb) is precisely that evaluated from the discrete spectrum. Also shown are length (upper cap) and velocity (lower cap) calculations by Bell and Kingston (1971), and RPA calculations by Amusia *et al*. (1976a). Not shown are calculations by Stewart (1978) from IP – 58.6 eV, which fall very close to the experimental curve. The gap ~60 eV is the region of prominent resonances. This is the only spectral region where experimental accuracy appears to exceed that of calculations, although the results of Stewart are very slightly higher. At lower energies, the length form of Bell and Kingston agrees better with experiment, as they anticipated. The RPA values are larger than the experimental results below 60 eV, but are in good agreement above the double ionization threshold. The contributions to the sum rules, based on the experimental data, have been reported previously (Berkowitz, 1997b) and are included in Table 2.1.

b.2 Resonances, 60–72 eV The 'excess oscillator strength' in each resonance is represented by the expression

$$f_{xs} = \frac{mc^2}{2e^2}\sigma\rho^2\Gamma(q^2 - 1)$$

given by Codling *et al*. (1967). Here m and e are the mass and charge of the electron, c the velocity of light, σ is the continuum cross section and ρ is the